Surfactin-Triggered Small Vesicle Formation of Negatively Charged Membranes: A Novel Membrane-Lysis Mechanism

Sébastien Buchoux,* Joséphine Lai-Kee-Him,* Marie Garnier,* Pascale Tsan,§ Françoise Besson,† Alain Brisson,* and Erick J. Dufourc*

*UMR 5248 CBMN, CNRS–Université Bordeaux 1, ENITAB, IECB, Pessac, France; §UMR 5078 CNRS–Université C. Bernard Lyon 1, Lyon, France; and †UMR 5246 ICBMS, CNRS–Université C. Bernard Lyon 1, Lyon, France

ABSTRACT The molecular mode of action of the lipopeptide SF with zwitterionic and negatively charged model membranes has been investigated with solid-state NMR, light scattering, and electron microscopy. It has been found that this acidic lipopeptide (negatively charged) induces a strong destabilization of negatively charged micrometer-scale liposomes, leading to the formation of small unilamellar vesicles of a few 10s of nanometers. This transformation is detected for very low doses of SF (Ri = 200) and is complete for Ri = 50. The phenomenon has been observed for several membrane mixtures containing phosphatidylglycerol or phosphatidylserine. The vesicularization is not observed when the lipid negative charges are neutralized and a cholesterol-like effect is then evidenced, i.e., increase of gel membrane dynamics and decrease of fluid membrane microfluidity. The mechanism for small vesicle formation thus appears to be linked to severe changes in membrane curvature and could be described by a two-step action: 1), peptide insertion into membranes because of favorable van der Waals forces between the rather rigid cyclic and lipophilic part of SF and lipid chains and 2), electrostatic repulsion between like charges borne by lipid headgroups and the negatively charged SF amino acids. This might provide the basis for a novel mode of action of negatively charged lipopeptides.

INTRODUCTION

Membrane-lytic peptides are known to be used for both offensive (in venoms, for instance) and defensive purposes. They play a major role in the invertebrate class and have been isolated from a wide range of organisms (from insects (1) to humans (2)). Most of these peptides exhibit antimicrobial activity and are composed of relatively small linear polypeptides (<40 amino acids) structured in α-helix (mainly), β-sheet, or cystein-stabilized α-helix-β-sheet folds. They have been intensively studied to understand how they interact with lipid membranes. Two main mechanisms of induced membrane destabilization have emerged from literature: ''carpet'' (3) and ''barrel'' (4) models, both requiring a helix conformation of the lytic peptide and leading to detergent-like action or pore formation. On the other hand, lipopeptides constitute a relatively new interest in the antimicrobial peptides family. The main difference between lipopeptides and more classical lytic peptides is the presence of a carbonated chain in complement to the peptidic backbone. Most described peptides (mainly from *Bacillus* species), include polymyxin (5), iturin (6), fengycin (7), and SF (8). SF is secreted by *Bacillus subtilis* and was discovered in the late 1960s (8). It was named after its ability to lower water surface tension from 72 mN/m to 27 mN/m (9). The morphology of SF is quite unusual because it is composed of a ring-shaped peptidic backbone of seven amino acids in a chiral sequence of L/D enantiomers: LLDLLDL. The ring is closed by a β-hydroxy fatty acid with different aliphatic chains (Fig. 1) (9). The amino acid sequence of the peptidic ring may differ according to genetic methods and/or strand used for biosynthesis (10), but in all cases it is composed of five lipophilic amino acids and two negatively charged hydrophilic ones (glutamic and aspartic acids) (8,11). Depending on the strand, the length of the hydrocarbon chain may also vary from 12 to 14 carbon atoms. Because of the presence of both a lipophilic and a hydrophilic part, SF exhibits powerful surfactant capabilities such as emulsification and foaming (8,12). SF also has interesting biological properties: it inhibits fibrin clot formation (8,13) and is quite an efficient antibacterial (14), antimycoplasmic (15), antitumoral (16–18), antiviral (19), and hypocholesterolemic (20) agent. Given these properties, SF has been proposed to be used to ensure safety of pharmaceutical products (15,21). Despite this impressive array of activities, only a few structural studies have been made: the structure of SF in dimethylsulfoxide solution or in detergent micelles is known (22,23) and has given a few clues on the mechanisms of interactions between SF and its multiple targets, but no major issue has risen concerning the minute mechanism for interactions. In particular, its mode of action toward biological membranes is still poorly understood. Computational studies and compression isotherms on a Langmuir trough have proposed that

Submitted January 1, 2008, and accepted for publication May 14, 2008.

Address reprint requests to Erick J. Dufourc, UMR 5248 CBMN, IECB, 2 rue Robert Escarpit, 33607 Pessac, France. Tel./Fax: 33-540002218; E-mail: e.dufourc@iecb.u-bordeaux.fr.

Abbreviations used: SF, surfactin; DLS, dynamic light scattering; TEM, transmission electron microscopy; DMPC, dimyristoylphosphatidylcholine; DMPG, dimyristoylphosphatidylglycerol; SM, sphingomyelin; DMPS, dimyristoylphosphatidylserine; PC, phosphatidylcholine; PG, phosphatidylglycerol; PS, phosphatidylserine; Ri, lipid/peptide molar ratio; S_{CD}, carbon-deuterium order parameter of deuterated chains; SUV, small unilamellar vesicle.

Editor: Lukas K. Tamm.

0006-3495/08/10/3840/10 $2.00

doi: 10.1529/biophysj.107.128322

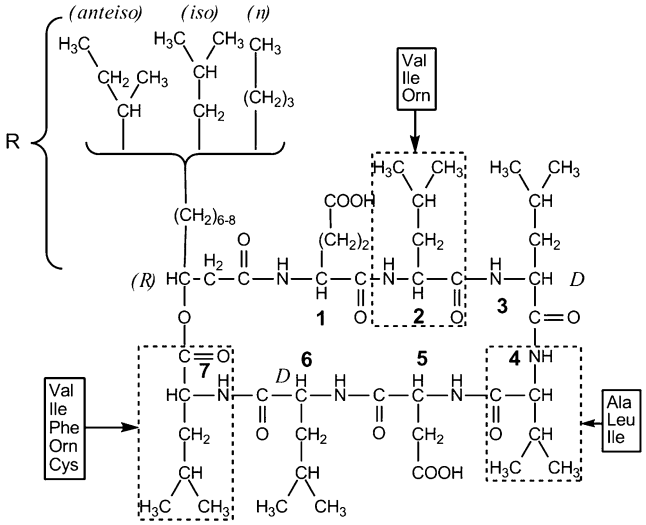

FIGURE 1 SF primary structure from Peypoux et al. (9). Alkyl chain in position 8 and amino acids at positions 2, 4, and 7 are variable depending on isoforms. Structure for the this study: ^{1}Glu(*L*)Leu(*L*)Leu(*D*)Val(*L*)Asp(*L*)Leu(*D*)Leu(*L*)^{7}-*iso*C_{14}, MW 1036.34.

SF may form clusters of seven monomers when interacting at the air/water interface (24), and a detergent-like effect on zwitterionic lipid model membranes has been reported from calorimetric studies at very elevated doses of SF (25–27), but interactions between SF and charged lipid membranes (such as *Mycoplasma* membranes) are still unknown.

Our purpose was to better understand the interaction mechanism by which SF induces the lysis of natural membranes. In this work, solid-state deuterium and phosphorus-31 NMR (^{2}H-NMR, ^{31}P-NMR), DLS, and TEM have been used to study the effect of SF against model membranes mimicking microorganism plasma membranes. In particular, three different systems have been investigated: DMPG/SM mixture (1:1 molar ratio), DMPC/DMPG mixture (1:1 molar ratio), and DMPC/DMPS mixture (1:1 molar ratio). These systems provide a good variety in lipid dynamics (SM is well known to be involved with cholesterol in rigid domain formation (28,29) as well as in lipid headgroup charge (PC and SM are both zwitterionic, whereas PG is anionic). PS is an interesting lipid because it is zwitterionic below pH 5 and negatively charged at pH 7. A DMPG/SM system may also be representative of *Mycoplasmas* lipid membrane composition (30) and so can be used to study biological properties of SF on a simplified model. Pure DMPC bilayers have been also used as a zwitterionnic model membrane. To enable ^{2}H NMR spectroscopy, lipids were (partially) deuterium labeled. When necessary, lipid structural and dynamic properties were determined by calculation of spectral moments and of S_{CD}.

MATERIALS AND METHODS

Chemicals

Brain SM, DMPG, DMPS, DMPC, DMPC-$^{2}H_{27}$, and DMPG-$^{2}H_{27}$ were purchased from Avanti Polar Lipids (Birmingham, AL) and used without further purification. SF (^{1}GluLeuLeuValAspLeuLeu^{7}-*iso*C_{14}, MW = 1036.34; Fig. 1) and other reagents were purchased from Sigma-Aldrich (St. Louis, MO). SF was checked for purity by mass spectrometry. Deuterium-depleted water was obtained from Eurisotop (Saint Aubin, France).

Multilamellar vesicle preparation

Except for the DMPC-$^{2}H_{27}$ system, all lipid systems were first dissolved in an organic solvent (chloroform) to achieve complete mixing of lipids. The organic solvent was then evaporated, and lipids were dried under high-vacuum pumping during several hours. To remove residual chloroform, the sample was hydrated with a large excess of water and highly vortex mixed before being freeze-dried. Finally, a 50 mM Tris-HCl buffer solution was added to lipids to reach 90% hydration (mass water/total mass) for NMR experiments (~350 mM). Formation of homogeneous multilamellar vesicles wass achieved with three to four freeze-thaw-mixing cycles: after being frozen in liquid nitrogen, sample was incubated for 10 min at 50°C (i.e., well above the ''gel-fluid'' transition temperature of all systems) and vortex mixed. Sample was then transferred into a 4-mm (~80 μL) NMR rotor for wide line experiments. For DLS, it was diluted 100 times and transferred into a 5-mm-diameter tube (250 μL, 3.5 mM). In the case of TEM experiments, an additional dilution was performed to reach a concentration of 1 mM; a 5-μL volume was then deposited on the carbon-coated copper grid. For SF-containing systems, SF powder was added to lipids before sample dissolution in chloroform; SF and lipids were then homogeneously mixed through dissolution in organic solvent. Sample preparation as described above was then applied. SF/lipid molar ratios of 25, 30, 50, 100, and 200 were prepared. Complementary experiments were also performed with external addition of SF as a buffer micellar solution (millimolar concentrations, i.e., well above the critical micelle concentration, which is a few micromolar) to already-prepared lipid solution. Equilibrium was also ensured using several freeze-thaw-vortex mixing cycles.

NMR spectroscopy

NMR experiments were carried out on Bruker Avance (Wissembourg, France) DSX 500 WB US (11.75 T) operating at 76.8 MHz for ^{2}H-NMR, DPX 400 NB US (9.4 T) operating at 161.9 MHz for ^{31}P-NMR, and DSX 300 WB US (7.05 T) operating at 46.1 MHz for ^{2}H-NMR. Pulse sequences used are a classical quadrupolar solid echo 90°x-τ-90°y-τ-acq (31) for ^{2}H-NMR and a Hahn-echo proton-decoupled for ^{31}P-NMR (32,33). Interpulse delays, τ, ranged from 30 μs at 11.75 T and 9.4 T to 50 μs at 7.05 T. A recycle delay of 1.5 s was used on both spectrometers for ^{2}H-NMR. It was set to 5 s for ^{31}P-NMR. All acquisitions were summed over 2K scans and detected using phase quadrature. A 30-min thermal equilibrium delay was waited before starting each experiment; temperature was regulated to ±0.1°C.

DLS

DLS experiments were performed on an ALV/CGS-3 goniometer, coupled with ALV/LSE-5003 electronics. Hydrodynamic radii were calculated using ALV-Correlator Software V. 3.0 fitting routines. Hardware and software are both from ALV-GmbH (Langen, Germany). All DLS experiments were performed at room temperature (~23°C), and samples used were the same as those used for ^{2}H-NMR, except they were diluted 100 times to be in the elastic collision range.

TEM

To prepare the TEM samples, 5 μL of an aqueous solution of the different preparations was deposited on a carbon-coated copper grid, which was rendered hydrophilic by UV/ozone treatment. Excess lipid solution was gently removed using absorbent paper. Samples were then negatively stained with a 2% uranyl acetate solution. TEM images were recorded using a CM 120 Philips Cryo transmission electron microscope operating at 120 kV and equipped with a USC1000 SSCCD 2k × 2k Gatan camera.

Cryo-TEM

A 5-μL sample was deposited onto a holey carbon-coated copper grid. The excess was blotted with a filter paper. Unstained samples were frozen into liquid ethane, and the grids mounted on a Gatan 626 cryoholder were transferred into the microscope and kept at a temperature near −175°C. Sample observations were performed with a Tecnai-F20 FEI-transmission electron microscope, operating at 200 kV. Low-dose images were recorded at a nominal magnification of 29,000× with a 2k × 2k USC1000 slow-scan CCD camera (Gatan, Pleasanton, CA).

Theoretical background and calculations

^{2}H-NMR has been widely used to provide information about structure and molecular motions in model membranes (34–36). Phospholipids involved in fluid-phase biomembranes can generally be described as a smectic-like liquid crystal and undergo rapid axially symmetrical reorientational motions around the bilayer normal. Because of this axial motion, structural properties of lipid chains can be described in terms of orientational order parameters. In particular, a carbon-deuterium orientational order parameter, S_{CD}, can be used to relate the observed quadrupolar splitting,$\Delta\nu$, to lipid motions (34–36):

$$\Delta\nu(\theta) = \frac{3}{2} \times A_Q \times \frac{3\cos^2\theta - 1}{2} \times S_{CD}, \quad (1)$$

where $A_Q = e^2qQ/h$ is the static deuterium quadrupolar coupling constant (167 kHz for C-^{2}H bonds (37)). θ is the angle between the bilayer normal and the magnetic field. S_{CD} is a time average over the molecular motions that are fast on the NMR time scale (i.e., compared with $\Delta\nu$). The carbon deuterium bond order parameter of the ith aliphatic chain segment is written as:

$$S^i_{CD} = \frac{1}{2} \times \langle 3\cos^2\beta_i - 1 \rangle, \quad (2)$$

where β_i is the angle between the C_i-^{2}H bond and the motional axis of symmetry (bilayer normal). Equations 1 and 2 may be applied to every ^{2}H nuclei in the molecule. Because multilamellar vesicles do not orient in the magnetic field, one generally observes a powder spectrum representative of all angle distributions: all θ -values are possible (generally 0 to 360°). When using perdeuterated chains, as in this work, one obtains a superposition of powder patterns originating from individual C_i-^{2}H bonds (i = 2–14). To gather information about minute chain dynamics (i.e., get individual S^i_{CD}), powder spectra are processed using the ''de-Pake-ing'' procedure (implemented by Bloom and colleagues (38,39)) to get rid of the θ angle distribution. By doing so, one obtains an oriented-like spectrum (choosing $\theta_{depak} = 90°$ for instance) and S^i_{CD} can directly be extracted from $\Delta\nu^i_Q$:

$$\Delta\nu^i(\theta_{depak}) = \Delta\nu^i_Q = \frac{3}{4} A_Q \times S^i_{CD}. \quad (3)$$

S^i_{CD} calculations presented in this article were performed using a PYREX/PYTHON program (S. Buchoux, unpublished material) based on the Sternin algorithm (39). Unfortunately, in dealing with experimental spectra, determination of $\Delta\nu^i_Q$ may be difficult because of low S/N or nonaxially symmetric spectra. A more global estimate of entire chain ordering may be obtained from spectral moments (34,40) such as the first moment M_1:

$$\langle S_{CD} \rangle_{chain} = \frac{\sqrt{3}}{\pi A_Q} M_1. \quad (4)$$

Angular brackets were used to represent the average over all labeled positions. The first moment is defined as:

$$M_1 = \frac{4\pi}{3\sqrt{3}} \langle \Delta\nu_Q \rangle = \frac{\int_{-\infty}^{\infty} \omega f(\omega) d\omega}{\int_{-\infty}^{\infty} f(\omega) d\omega}. \quad (5)$$

Where $\omega = 0$ corresponds to the isotropic frequency. First moments were calculated using a Python homemade routine to which Bruker NMR data were exported using a proper subroutine (S. Buchoux, unpublished material). To avoid zero values for spectra symmetrical relative to the origin, a sign reversal was used for negative frequencies.

RESULTS

Deuterium and phosphorus solid-state NMR experiments were performed as a function of temperature on several lipid mixtures: DMPC-$^2H_{27}$ liposomes, DMPG-$^2H_{27}$/SM (1/1) liposomes, DMPC-$^2H_{27}$/DMPG (1/1) liposomes, and DMPC-$^2H_{27}$/DMPS (1/1) liposomes. Each system was analyzed with and without incorporated SF (Ri of 25, 30, 50, 100, and 200). DLS and TEM experiments were performed only on systems of interest characterized by NMR.

^{2}H NMR spectroscopy

Fig. 2 shows ^{2}H-NMR spectra of the DMPC-$^2H_{27}$ system with and without SF at three characteristic temperatures (18°C, 21°C, and 39°C) within the temperature range investigated (18–48°C). Acquisition conditions were kept identical for all experiments. In the case of pure DMPC-$^2H_{27}$ liposomes (Fig. 2, *left*), we observe the typical behavior of this well-studied system (34,35,41,42). At 18°C and 21°C, DMPC chains are not melted (i.e., thermally activated motions are not fast enough to induce molecule and chain disorder); the spectrum observed is characteristic of a lamellar gel phase: there is no fast axial rotation of lipid (no C_3 axis symmetry), and chains are essentially fully extended with an ~30° tilt (43). A very small isotropic line caused by either

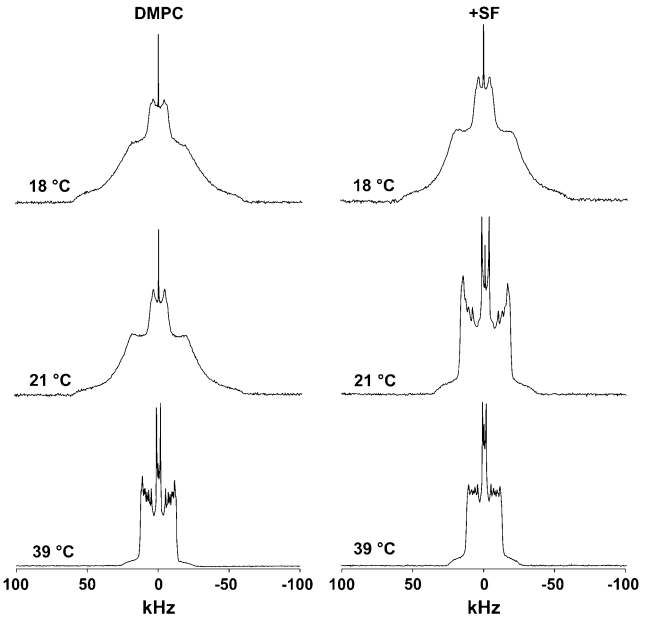

FIGURE 2 SF effect on DMPC-$^2H_{27}$ MLV (20 mg in 100 μL). ^{2}H-NMR spectra are shown at 18°C, 21°C, and 39°C, in the absence of SF (*left*) and with SF incorporated (Ri = 25, *right*). Number of acquisitions = 2k, 50-Hz Lorentzian filtering.

residual natural abundance water or by very small vesicles occurring during the preparation is observed; it can be neglected because of its weak area (<1%). The spectrum observed at 39°C is characteristic of a lamellar fluid phase: lipids undergo fast axially symmetric motions (molecule long axis rotation and wobbling, chain rotation, chain isomerization), which result in liquid-like chain disordering. The temperature transition between gel and fluid phase occurs between 21°C and 24°C, which agrees with the literature: for DMPC, the phase transition is 23.5°C (44) (here it is slightly lower because chains are perdeuterated (28)). In the presence of SF (Ri = 25) (Fig. 2, *right*), no characteristic changes in spectrum shape occur at 18°C. The effect is much more visible at 21°C because the gel phase spectrum evolves toward a fluid phase with SF addition. Very little change is observed at 39°C: the same spectrum width but with a small line broadening. First moment calculations (not shown) also reveal that there are no large changes in DMPC membrane dynamics in the presence of SF: M_1 is high at low temperatures (~100 kHz at 18°C) and is lower at high temperatures (~40 kHz at 39°C). From the temperature variation of M_1 (not shown) one can determine a gel-to-fluid phase transition temperature of 22 ± 1°C in the absence of SF and one of 20 ± 1°C in its presence.

Fig. 3 (*four top spectra*) shows ^{2}H-NMR of DMPG-$^2H_{27}$/SM system without (*left*) and with (*right*) SF at two temperatures (18°C and 39°C) within the temperature range investigated (18–48°C). For the DMPG-$^2H_{27}$/SM only system, we observe a gel phase spectrum at 18°C and 39°C that is related to the well-known effect of SM as a promoter of increase in the transition temperature between gel phase and fluid phase (29). Indeed, transition begins to be observed at 48°C, which is twice as high as for the DMPG-only system (44) (spectrum not shown). Negligible isotropic lines are also observed independent of temperature. When SF is added to the system (Ri = 50), we observe a complete conversion of spectra into isotropic lines at both temperatures. The SF effect on DMPG-$^2H_{27}$/SM system is remarkable because the lamellar phase spectrum has completely vanished. The four bottom spectra of Fig. 3 report on ^{2}H-NMR of DMPC-$^2H_{27}$/DMPG system without (*left*) and with (*right*) SF at 18°C and 39°C within the temperature range investigated (18–48°C). For the DMPC-$^2H_{27}$/DMPG system, we observe a gel-phase spectrum at 18°C but a fluid-phase spectrum at 39°C. Again, negligible isotropic lines are observed at low and high temperatures. When SF is added to the system, a pure isotropic spectrum is observed at 18°C, as for the DMPG/SM membrane. Interestingly, a small fraction of powder pattern remains visible at 39°C, the isotropic line nonetheless being dominant (~85% of the total spectrum area). Fig. 4 shows ^{2}H NMR spectra of DMPC-$^2H_{27}$/DMPS system without (*left*) and with (*right*) SF at two typical temperatures (18°C and 39°C) within the temperature range investigated (18–48°C) and at two different pHs (pH = 4.5, *bottom*, and 7.5, *top*). Acquisition conditions were kept identical for all experiments. Without SF (*left*), spectra observed are quite similar at pH = 4.5 and at pH = 7.5: spectra observed at 18°C are characteristic of a gel phase, whereas at 39°C they are characteristic of a fluid phase. Negligible isotropic lines are also observed. When SF is added to the system (*right*), spectra show marked differences: at pH = 4.5, lamellar phase spectra are always observed (at both 18°C and 39°C), whereas at pH = 7.5, an isotropic spectrum is detected independent of temperature. More detail on the pH = 4.5 system may be obtained by calculating the first spectral moment, M_1, of DMPC-$^2H_{27}$ lipid chains (Fig. 5). Without SF, a phase transition between gel and fluid phases is clearly visible because of the marked step in the M_1 profile on going from low temperatures (high M_1 values (~120 kHz), ordered chains) to high temperatures (lower M_1 values (~40 kHz), disordered chains). In the presence of SF, M_1 is lowered (~100 kHz) at low temperatures and is increased (~50 kHz) at high temperatures; as a consequence, the phase transition is less visible. The S_{CD} scale on the right-hand side *y* axis reflects the M_1 behavior on a scale between 1 (full order, rigid lipids and chains) and 0 (full disorder, as in liquids). The Fig. 5 insert shows the so-called ''order parameter profile,'' obtained from DMPC-$^2H_{27}$ ''de-Paked'' spectra in DMPC/DMPS at 34°C, in the presence and absence of SF. It is clearly seen that DMPC-$^2H_{27}$ chain order is much higher when SF is present in

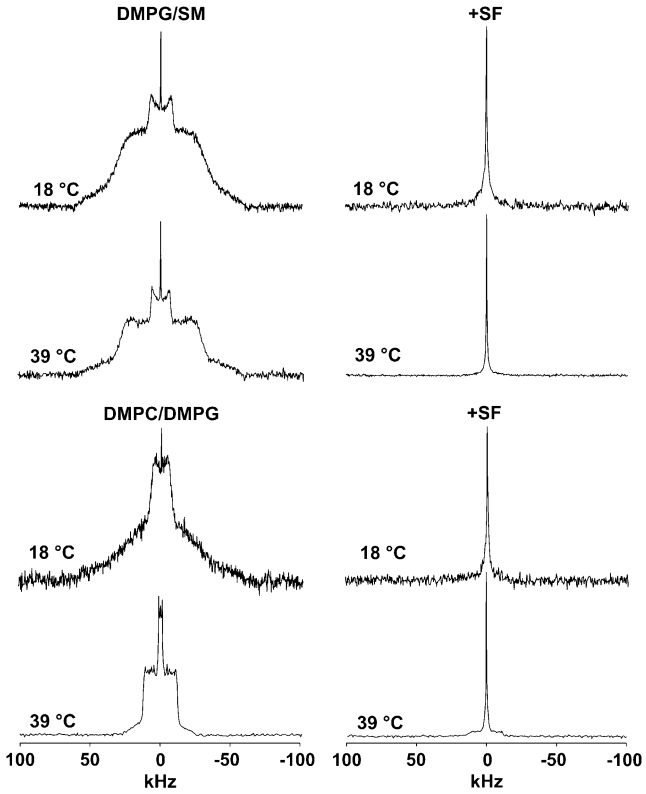

FIGURE 3 SF effect on DMPG-$^2H_{27}$/SM (1:1 molar ratio) and DMPC-$^2H_{27}$/DMPG (1:1 molar ratio) systems (20 mg total lipids in 100 μL). ^{2}H-NMR spectra are shown at 18°C and 39°C, in the absence (*left*) and in the presence of SF (*right*, Ri = 50). NMR conditions as in Fig. 2.

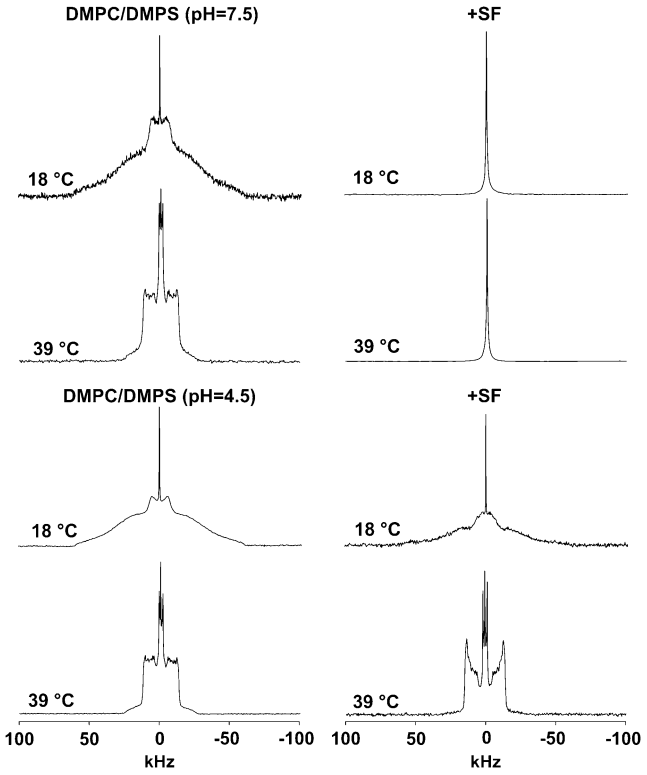

FIGURE 4 SF effect on DMPC-$^2H_{27}$/DMPS (1:1 molar ratio) system at pH 7.5 (*top*) and pH 4.5 (*bottom*), (20 mg total lipids in 100 μL). ^{2}H-NMR spectra are shown at 18°C and 39°C, in the absence (*left*) and in the presence of SF (*right*, Ri = 50). NMR conditions as in Fig. 2.

the system. This is especially true for ''plateau'' positions (carbons 2 to 8) and down to position 11. Toward the chain end (positions 12 to 14), the effect is less marked or absent (methyl terminal).

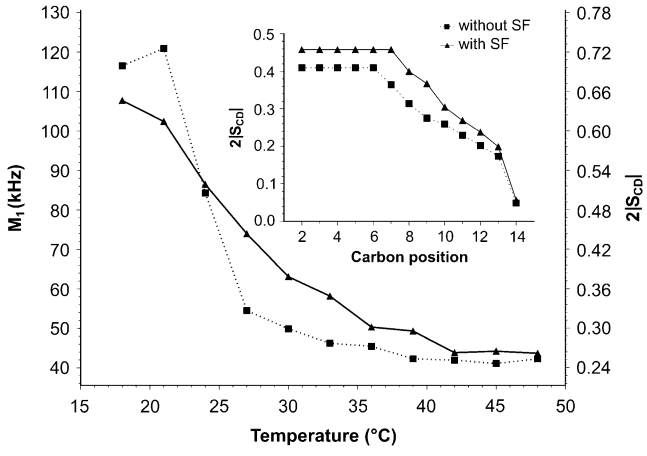

FIGURE 5 Temperature dependence of M_1 calculated for DMPC-$^2H_{27}$/DMPS (1:1 molar ratio) spectra at pH 4.5 without SF (*squares*) and with SF (Ri = 50, *triangles*). (*Inner graph*) S_{CD} profile calculated for de-Paked spectra (see text) at T = 34°C. Labeled carbon positions were assigned according to the literature. Experimental error is in symbol size.

^{31}P NMR Spectroscopy

The effect of lower doses of SF on negatively charged membrane systems was performed on DMPC/DMPG using ^{31}P NMR spectroscopy because it does not require labeled materials. Fig. 6 shows the effect of increasing doses of SF (lipid/peptide ratios of 200, 100, and 50) at 39°C and 18°C. In the absence of peptide, one observes the classical axially symmetric spectra at both temperatures. This is at variance to what is observed with deuterium NMR because of the still rotating phosphate headgroup, even in the gel phase. Axially asymmetric spectra characteristic of frozen headgroup motions are observed only at very low temperatures (35,45). Gel- and fluid-phase spectra nonetheless show very distinguishable shapes because of the frequency increase of molecular and intramolecular motions above the phase transition. Because the chemical shift anisotropies of each of the lipid headgroups (PC and PG) are about the same, and only one axially symmetric powder spectrum is observed. Very weak and negligible isotropic lines are detected and may be assigned to the formation of a very small amount (<1%) of very small vesicles. In the presence of SF, a single isotropic line centered close to 0 ppm is detected, and the more SF the greater is the line. At Ri = 50, the powder pattern characteristic of micrometer-size multilayered vesicles has almost completely disappeared, as was seen with deuterium NMR (vide supra). The line appears independent of the temperature and, although weak, for very low proportions of peptide.

DLS experiments

DLS experiments were performed on DMPC/DMPG and DMPC/DMPS (at pH = 7.5) to measure the size of the isotropic objects detected with NMR. Fig. 7 shows the effect of

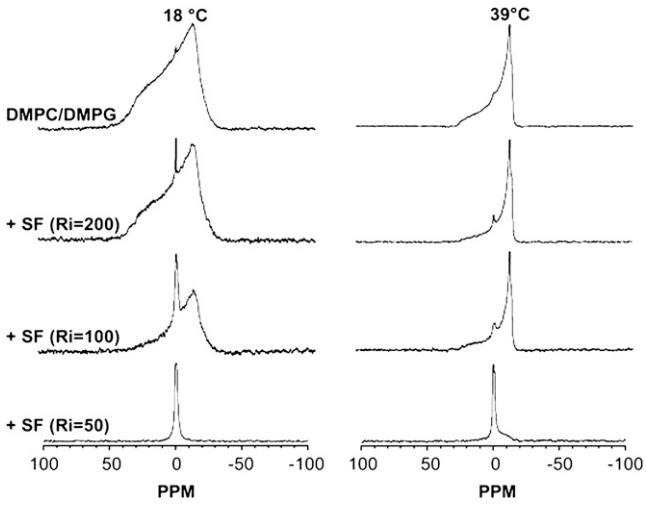

FIGURE 6 SF effect on DMPC/DMPG (1:1 molar ratio) systems (20 mg total lipids in 100 μL). ^{31}P-NMR spectra are shown at 18°C and 39°C, with increasing amounts of SF from top to bottom. Number of acquisitions = 1k, 50-Hz Lorentzian filtering.

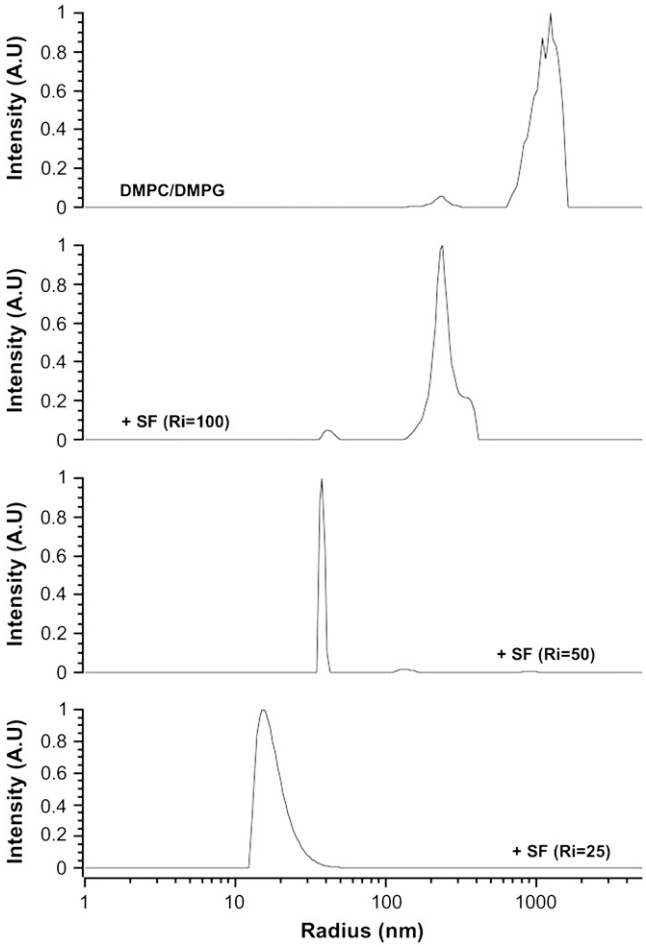

FIGURE 7 Effect of SF on the hydrodynamic radius of DMPC/DMPG (1:1 molar ratio) MLV, as monitored by DLS. Lipid/peptide molar ratios are shown on graphs. Temperature was regulated at 25°C.

increasing amounts of SF on the hydrodynamic radius, Rh, of DMPC/DMPG MLV at room temperature (23°C). Heterogeneous sizes centered on Rh ≈ 1000 nm are mostly detected in the absence of peptide. A small proportion of smaller objects with Rh ≈ 220 nm are also observed. This accounts well for the small proportion of isotropic lines detected on top of NMR powder spectra. On addition of SF, Ri = 100 (Fig. 7), the system is almost entirely converted into objects of Rh ≈ 220 nm. A small proportion of smaller sizes are also detected (Rh ≈ 40 nm). With Ri = 50, the population with Rh ≈ 35 nm dominates, with a very narrow distribution (± 2 nm). For Ri = 25, even smaller objects are detected, Rh ≈ 15 nm, with a ±5 nm asymmetric size distribution. Similar observations are made for DMPC/DMPS at pH = 7.5 (not shown).

TEM

After the preparation outlined in Materials and Methods, electron microscopy images were taken on the system DMPC/DMPG with and without SF (Fig. 8). Control ex-

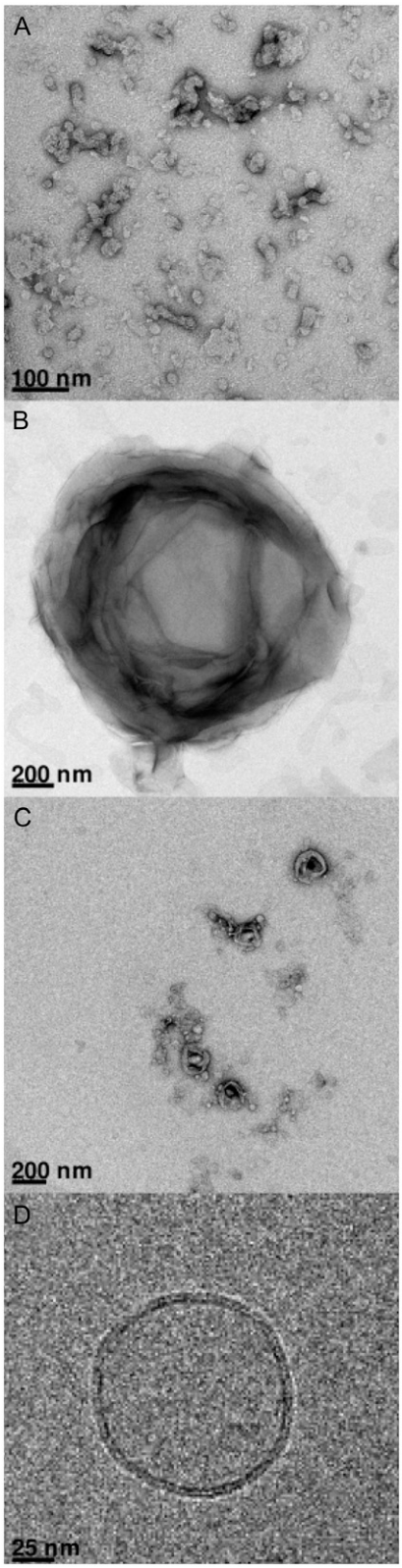

FIGURE 8 TEM images of SF and of DMPC/DMPG (1:1 molar ratio) without and with lipopeptide, using negative staining (*A*, *B*, and *C*) and cryo-TEM (*D*). (*A*) SF micelles, bar: 100 nm. (*B*) MLV in the absence of peptide, bar = 200 nm. (C) With SF, Ri = 50, bar: 200 nm. (*D*) Same as *C* observed using cryo-TEM, bar: 25 nm.

periments were also taken on a pure SF micellar dispersion Fig. 8 *A*: micelles of 10–50 nm size are observed because the dispersion is well above the CMC (a few micromolar). DMPC/DMPG liposomes were also imaged, and the classical ''onion-like'' structure of micrometer size was observed (Fig. 8 *B*). It is clear that on addition of small amounts (Ri = 50, Fig. 8 *C*) of SF, the morphology and size of the initially observed micrometer multilamellar vesicles is considerably modified: vesicles of ~100–200 nm are observed. Additional Cryo-TEM experiments were performed and established that virtually all vesicles formed when SF is added are unilamellar (Fig. 8 *D*), with a bilayer thickness estimated to be ~5 nm. External addition of SF as a micellar water solution (6 mM) to preformed MLV (not shown) leads to the same final state as observed in Fig. 8, where the peptide was codissolved with lipids and membranes formed after solvent evaporation, lyophilization, and rehydration (see Materials and Methods).

DISCUSSION

Three major findings emerge from our NMR, DLS, and TEM experiments. 1), Very low doses of SF lead to transformation of large membrane dispersions into small unilamellar vesicles. 2), Part of the mechanism is clearly driven by electrostatic repulsion because it occurs only on negatively charged systems and independent of the physical state of the lipid. 3), The SF has a cholesterol-like action on membranes when the electrostatic interaction is diminished or cancelled. These results are presented in detail and discussed in the following sections.

Transformation of MLV into SUV

A lipid/SF ratio of 50 (~4 mol % of SF) almost entirely converts multilamellar vesicles of micrometer size into small spherical objects of ~70 nm. This is detected by the appearance of an isotropic line in ^{2}H-NMR spectra: i.e., the newly formed small objects undergo fast tumbling that averages to zero the large quadrupolar interaction. This has been observed on several membrane systems: DMPC-$^2H_{27}$/DMPG, DMPG-$^2H_{27}$/SM, and DMPC-$^2H_{27}$/DMPS (at pH = 7.5). Small objects formation has been confirmed by DLS because no micrometer-scaled vesicles are observed on SF addition. Interestingly, a lipid/peptide ratio of 50 appears to be sufficient to transform almost the entire MLV into a narrow population of vesicles. Smaller particles (e.g., mixed micelles, very small vesicles) are formed on increasing the amount of SF (diameter of ~30 nm for Ri = 25), whereas lower doses of SF (Ri = 100 or 200) lead to larger vesicles (400–500 nm). The observation of a dose-dependent size transformation is also confirmed using ^{31}P-NMR: only a small fraction of isotropic line superimposed on a powder pattern is observed at high Ri. Interestingly, at low and high doses, the population of vesicles is heterogeneous in size, whereas it is very narrow at Ri = 50. Additionally, TEM experiments on negatively stained DMPC/DMPG vesicles without SF and with Ri = 50 also demonstrate SF-induced formation of small objects, presumably small unilamellar vesicles. Complementary cryo-TEM experiments clearly establish that these small objects are unilamellar vesicles, with a bilayer thickness of ~5 nm. SF-induced multilamellar vesicles destabilization is quasi-independent of the physical state of lipids. It indeed happens on the low- and high-temperature phases of DMPC/DMPG or DMPC/DMPS systems and on DMPG/SM systems that are in a very ordered gel-like phase at both ambient and 40–50°C temperatures. The fact that lipid chains are in a liquid-disordered or solid ordered phase appears not to be an important parameter for the interaction. This is in contrast with other lysis-inducing peptides, such as the bee-venom melittin, where small particles are preferentially formed with rigid chain lipids (46–50). DLS and electron microscopy confirm that objects of 70-nm size are thus formed on action of SF on these systems. TEM clearly demonstrates that with Ri = 50 small unilamellar vesicles are stabilized. Interestingly, an Ri of 50 appears to be sufficient to transform almost the entire MLV entirely into a narrow population of vesicles. Smaller particles are formed on increasing the amount of SF (diameter of ~30 nm for Ri = 25), whereas lower doses of SF (Ri = 100 or 200) lead to larger vesicles (400–500 nm). The observation of a dose-dependent size transformation is also confirmed using ^{31}P-NMR: only a small fraction of isotropic line superimposed on a powder pattern is observed at high Ri. Interestingly, at low and high doses, the population of vesicles is heterogeneous in size, whereas it is very narrow at Ri = 50. From our results, it is clear that a considerable effect is induced by SF on negatively charged membrane systems of different lipid nature. Effects of SF on both biological systems (16,19) and model systems (25–27,51,52) have already been reported, but the doses applied were much higher. In particular, recent ^{2}H- and ^{31}P-NMR studies (26,27) performed on POPC reveal a complete membrane disruption for a lipid/SF ratio of ~4. This suggests that for high doses, the ''wedge'' shape of SF may exert a destabilizing effect in the absence of any electrostatic action. Experiments have been reported on phosphatidylethanolamine and negatively charged lipids (DMPG) by calorimetry and x rays. A deep insertion of SF and bilayer stabilization were observed (52); unfortunately, the techniques used did not allow detection of small vesicles.

Electrostatic repulsion as the key interaction

It appears rather clear that repulsion between SF negative charges (Asp and Glu residues) and DMPG headgroup negative charge lead to formation of SUVs. Interestingly, SUVs occur with DMPC/DMPS at pH = 7.5 but not at pH = 4.5. DMPS is indeed an interesting lipid because its headgroup charge is dependent on pH (44). At pH = 4.5, the carboxylic acid function of a serine headgroup is protonated, and amino and phosphate groups are still charged (respectively positively and negatively); as a consequence, DMPS is then

zwitterionic, leading to a globally neutral membrane (53). At pH = 7.5, DMPS is anionic because its carboxylic acid function is deprotonated. As a consequence DMPC-$^2H_{27}$/DMPS liposomes are negatively charged. Because SF is also negatively charged at pH = 7.5, we may also explain the formation of DMPC-$^2H_{27}$/DMPS SUV by charge repulsions. In contrast, at pH = 4.5, the PS headgroup is protonated and globally neutral so the DMPC-$^2H_{27}$/DMPS membrane is zwitterionic. Although SF may still be negatively charged at pH = 4.5 (54), no SUV formation is observed at such pH because there are no longer charge repulsions between SF and the PS headgroup. The partial protonation of carboxyl groups would even allow the whole peptide to insert into the lipid in a way similar to that of cholesterol (vide infra).

SF and lipids dynamics

When the membrane system is not converted into small objects on SF action, i.e., in the presence of zwitterionic membranes, one observes powder patterns with NMR and therefore, a minute analysis of membrane dynamics may be carried out from the deuterium NMR data. Concerning the DMPC system, no crucial effect is observed when SF is added to it, except for a broadening and lowering of the gel-to-fluid phase transition: at 21°C the ^{2}H-NMR spectrum observed with SF is much closer to a fluid phase spectrum, whereas it is mostly of gel-type for pure DMPC-$^2H_{27}$. Results obtained with DMPC-$^2H_{27}$/DMPS system at pH 4.5 reveal that SF at Ri = 50 lowers lipid chain order at low temperature and raises it at high temperature, leading to broadening of the gel-to-fluid phase transition. Of interest is the fact that the acyl chain ordering increases in the fluid phase for almost all positions except for the methyl terminal. This effect is very similar to what is observed with cholesterol in membranes, except that cholesterol also orders the chain ends (40,42,43,55,56). We may account for this behavior by a deep insertion of SF into the bilayer core. In the presence of rigid chains (gel phase), SF will prevent close packing of chains and then alter phase transition phenomena and membrane ordering, whereas on a fluid phase, the peptide rigid ring may to some extent play the same role as the fused rings of cholesterol, i.e., increasing Van der Waals interactions and promoting membrane ordering. The fact that the chain ends are less ordered suggests nonetheless that SF is less embedded than cholesterol in the bilayer. This cholesterol-like behavior, not observed with SF in pure DMPC-$^2H_{27}$ membrane, may be enhanced by interactions between the SF peptidic backbone and the DMPS serine headgroup, as proposed in the recent work using molecular dynamics to study SF/membrane interactions (57).

Proposed mechanism of action

Results presented in this article reveal that application of low doses of SF on negatively charged membranes promotes micrometric size membrane destabilization and leads to the formation of SUVs of a few 10s of nanometers. Additionally, this behavior is essentially driven by repulsions between negatively charged acidic residues from SF and negative charges located on the lipid headgroup (PG and PS at pH 7.5). Lipids dynamics does not seem to be an important issue concerning SF interactions with membranes because SUV formation occurs both with gel- and fluid-phase lipids. A hypothetical model for membrane morphological transformation (lysis) can be proposed based on these observations (Fig. 9). The first stage would be 1), a penetration of SF into the lipid bilayer because of a favorable hydrophobic interaction between SF and the membrane; 2), charge repulsions take place between SF negative charges and the lipid headgroup negative charges, which leads to local increase of membrane curvature; and 3), a complete destabilization of the planar membrane and formation of resulting SUVs. This is what is usually called ''direct lysis''; i.e., while the chemical integrity of the lipid is preserved, the membrane morphology is dramatically changed, leading to severe leakage of the liposome and, by extrapolation to microorganisms, to cell contents. Compared with the well-studied ''carpet'' and ''barrel'' models (58,59), our model presented here does not rely on helix conformation or presence of basic residues, as reported for many antibacterial peptides. Neither helical nor β-sheet structure can be adopted by SF because of its cyclic structure.

The presented mechanism may also apply to membrane direct lysis induced by other lipopeptides secreted by *Bacillus subtilis*. For example, it would be interesting to make similar experiments with the iturinic antibiotics (mycosubtilin, bacillomycins L and D), which are lipopeptides like SF but differ by their chiral sequence of L/D enantiomer amino acids (LDDLLDL instead of LLDLLDL in SF) and by the nature of the cycling fatty acid (β-amino fatty acid instead of β-hydroxy fatty acid in SF).

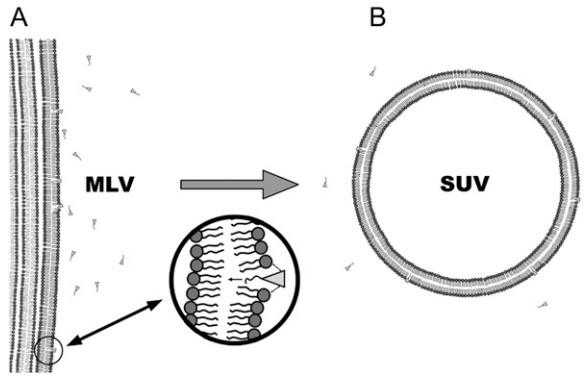

FIGURE 9 Artist view illustrating the ''wedge-repulsion'' model: SF molecules penetrate into the hydrophobic core of membranes because of favorable hydrophobic forces, and an electrostatic repulsion occurs between negative charges of peptidic amino acids Glu/Asp and negatively charged lipid headgroups. This promotes an increase in local membrane curvature, which destabilizes MLV (*A*) to form SUVs (*B*).

REFERENCES

1. Bulet, P., and R. Stöcklin. 2005. Insect antimicrobial peptides: structures, properties and gene regulation. *Protein Pept. Lett.* 12:3–11.
2. Agerberth, B., H. Gunne, J. Odeberg, P. Kogner, H. G. Boman, and G. H. Gudmundsson. 1995. FALL-39, a putative human peptide antibiotic, is cysteine-free and expressed in bone marrow and testis. *Proc. Natl. Acad. Sci. USA.* 92:195–199.
3. Pouny, Y., D. Rapaport, A. Mor, P. Nicolas, and Y. Shai. 1992. Interaction of antimicrobial dermaseptin and its fluorescently labeled analogues with phospholipid membranes. *Biochemistry.* 31:12416–12423.
4. Ehrenstein, G., and H. Lecar. 1977. Electrically gated ionic channels in lipid bilayers. *Q. Rev. Biophys.* 10:1–34.
5. Stansly, P. G., and M. E. Schlosser. 1947. Studies on polymyxin: isolation and identification of *Bacillus polymyxa* and differentiation of polymyxin from certain known antibiotics. *J. Bacteriol.* 54:549–556.
6. Delcambe, L. 1950. Iturine, new antibiotic produced by *Bacillus subtilis*. *C. R. Seances Soc. Biol. Fil.* 144:1431–1434.
7. Vanittanakom, N., W. Loeffler, U. Koch, and G. Jung. 1986. Fengycin–a novel antifungal lipopeptide antibiotic produced by *Bacillus subtilis* F-29–3. *J. Antibiot. (Tokyo).* 39:888–901.
8. Arima, K., A. Kakinuma, and G. Tamura. 1968. Surfactin, a crystalline peptide-lipid surfactant produced by *Bacillus subtilis*: isolation, characterization and its inhibition of fibrin clot formation. *Biochem. Biophys. Res. Commun.* 31:488–494.
9. Peypoux, F., J. M. Bonmatin, and J. Wallach. 1999. Recent trends in the biochemistry of surfactin. *Appl. Biochem. Biotechnol.* 51:553–563.
10. Kowall, M., J. Vaterb, B. Klugeb, T. Steinb, P. Frankec, and D. Ziessow. 1998. Separation and characterization of surfactin isoforms produced by *Bacillus subtilis* OKB 105. *J. Colloid Interface Sci.* 204:1–8.
11. Kakinuma, A., H. Sugino, M. Isono, G. Tamura, and K. Arima. 1969. Determination of fatty acid in surfactin and elucidation of the total structure of surfactin. *Agric. Biol. Chem.* 33:973–976.
12. Deleu, M., H. Razafindralambo Y. Popineau, P. Jacques, P. Thonart, and M. Paquot,. 1999. Interfacial and emulsifying properties of lipopeptides from *Bacillus subtilis*. *Colloid Surface A.* 152:3–10.
13. Kakinuma, A., G. Tamura, and K. Arima. 1968. Wetting of fibrin plate and apparent promotion of fibrinolysis by surfactin, a new bacterial peptidelipid surfactant. *Experientia.* 24:1120–1121.
14. Mannanov, R. N., and R. K. Sattarova. 2001. Antibiotics produced by *Bacillus* bacteria. *Chem. Nat. Compd.* 37:117–123.
15. Vollenbroich, D., G. Pauli, M. Ozel, and J. Vater. 1997. Antimycoplasma properties and application in cell culture of surfactin, a lipopeptide antibiotic from *Bacillus subtilis*. *Appl. Environ. Microbiol.* 63:44–49.
16. Kameda, Y., S. Oira, K. Matsui, S. Kanatomo, and T. Hase. 1974. Antitumor activity of *Bacillus natto*. V. Isolation and characterization of surfactin in the culture medium of *Bacillus natto* KMD 2311. *Chem. Pharm. Bull. (Tokyo).* 22:938–944.
17. Papo, N., M. Shahar, L. Eisenbach, and Y. Shai. 2003. A novel lytic peptide composed of DL-amino acids selectively kills cancer cells in culture and in mice. *J. Biol. Chem.* 278:21018–21023.
18. Kim, S. Y., J. Y. Kim, S. H. Kim, H. J. Bae, H. Yi, S. H. Yoon, B. S. Koo, M. Kwon, J. Y. Cho, C. E. Lee, and S. Hong. 2007. Surfactin from *Bacillus subtilis* displays anti-proliferative effect via apoptosis induction, cell cycle arrest and survival signaling suppression. *FEBS Lett.* 581:865–871.
19. Vollenbroich, D., M. Ozel, J. Vater, R. M. Kamp, and G. Pauli. 1997. Mechanism of inactivation of enveloped viruses by the biosurfactant surfactin from *Bacillus subtilis*. *Biologicals.* 25:289–297.
20. Tsukagoshi, N., G. Tamura, and K. Arima. 1970. A novel protoplast-bursting factor (surfactin) obtained from *Bacillus subtilis* IAM 1213: II. The interaction of surfactin with bacterial membranes and lipids. *Biochim. Biophys. Acta.* 196:211–214.
21. Nissen, E., G. Pauli, J. Vater, and D. Vollenbroich. 1997. Application of surfactin for mycoplasma inactivation in virus stocks. *In Vitro Cell. Dev. Biol. Anim.* 33:414–415.
22. Bonmatin, J. M., M. Genest, H. Labbé, and M. Ptak. 1994. Solution three-dimensional structure of surfactin: a cyclic lipopeptide studied by 1H-NMR, distance geometry, and molecular dynamics. *Biopolymers.* 34:975–986.
23. Tsan, P., L. Volpon, F. Besson, and J. M. Lancelin. 2007. Structure and dynamics of surfactin studied by NMR in micellar media. *J. Am. Chem. Soc.* 129:1968–1977.
24. Gallet, X., R. Brasseur, M. Deleu, H. Razafindralambo, M. Paquot, P. Jacques, and P. Thonart. 1999. Computer simulation of surfactin conformation at a hydrophobic/hydrophilic interface. *Langmuir.* 15:2409–2413.
25. Heerklotz, H., and J. Seelig. 2001. Detergent-like action of the antibiotic peptide surfactin on lipid membranes. *Biophys. J.* 81:1547–1554.
26. Heerklotz, H., and J. Seelig. 2007. Leakage and lysis of lipid membranes induced by the lipopeptide surfactin. *Eur. Biophys. J.* 36:305–314.
27. Heerklotz, H., T. Wieprecht, and J. Seelig. 2004. Membrane perturbation by the lipopeptide surfactin and detergents as studied by deuterium. *J. Phys. Chem. B.* 108:4909–4915.
28. Aussenac, F., M. Tavares, and E. J. Dufourc. 2003. Cholesterol dynamics in membranes of raft composition: a molecular point of view from 2H and 31P solid-state NMR. *Biochemistry.* 42:1383–1390.
29. Wang, T.-Y., and J. R. Silvius. 2003. Sphingolipid partitioning into ordered domains in cholesterol-free and cholesterol-containing lipid bilayers. *Biophys. J.* 84:367–378.
30. Hirai, Y., S. Kukida, O. Matsushita, E. Nagamachi, K. Tomochika, and Y. Kanemasa. 1992. Membrane lipids of *Mycoplasma orale*: lipid composition and synthesis of phospholipids. *Physiol. Chem. Phys. Med. NMR.* 24:21–27.
31. Davis, J. H., K. R. Jeffrey, M. Bloom, M. I. Valic, and T. P. Higgs. 1976. Quadrupolar echo deuteron magnetic resonance spectroscopy in ordered hydrocarbon chains. *Chem. Phys. Lett.* 42:390–394.
32. Dufourc, E. J., C. Mayer, J. Stohrer, and G. Kothe. 1992. P-31 and H-1-NMR pulse sequences to measure lineshapes, T1z and T2e relaxation-times in biological-membranes. *J. Chim. Phys.-Chim. Biol.* 89:243–252.
33. Rance, M., and R. A. Byrd. 1983. Obtaining high-fidelity spin-1/2 powder spectra in anisotropic media—phase-cycled Hahn echo spectroscopy. *J. Magn. Reson.* 52:221–240.
34. Davis, J. H. 1983. The description of membrane lipid conformation, order and dynamics by ^{2}H-NMR. *Biochim. Biophys. Acta.* 737:117–171.
35. Dufourc, E. J. 2006. Solid state NMR in biomembranes. *In* Chemical Biology. B. Larijani, R. Woscholski, and C. A. Rosser, editors. J. Wiley & Sons, London. 113–131.
36. Seelig, J. 1977. Deuterium magnetic resonance: theory and application to lipid membranes. *Q. Rev. Biophys.* 10:353–418.
37. Burnett, L. J., and B. H. Müller. 1971. Deuteron quadrupolar coupling constants in three solid deuterated paraffin hydrocarbons: C2D6, C4D10, C6D14. *J. Chem. Phys.* 55:5829–5831.
38. Bloom, M., J. H. Davis, and A. L. Mackay. 1981. Direct determination of the oriented sample NMR spectrum from the powder spectrum for systems with local axial symmetry. *Chem. Phys. Lett.* 80:198–201.
39. Sternin, E., M. Bloom, and A. L. MacKay. 1983. De-Pake-ing of NMR spectra. *J. Magn. Reson.* 55:274–282.
40. Beck, J. G., D. Mathieu, C. Loudet, S. Buchoux, and E. J. Dufourc. 2007. Plant sterols in ''rafts'': a better way to regulate membrane thermal shocks. *FASEB J.* 21:1714–1723.
41. Douliez, J. P., A. Leonard, and E. J. Dufourc. 1996. Conformational order of DMPC *sn*-1 versus *sn*-2 chains and membrane thickness: An approach to molecular protrusion by solid state H-2-NMR and neutron diffraction. *J. Phys. Chem.* 100:18450–18457.
42. Leonard, A., and E. J. Dufourc. 1991. Interactions of cholesterol with the membrane lipid matrix - a solid-state NMR approach. *Biochimie.* 73:1295–1302.
43. Leonard, A., C. Escrive, M. Laguerre, E. Pebay-Peyroula, W. Neri, T. Pott, J. Katsaras, and E. J. Dufourc. 2001. Location of cholesterol in DMPC membranes. A comparative study by neutron diffraction and molecular mechanics simulation. *Langmuir.* 17:2019–2030.

44. Cevc, G. 1993. Phospholipids Handbook. CRC Press, Boca Raton, FL.

45. Dufourc, E. J., C. Mayer, J. Stohrer, G. Althoff, and G. Kothe. 1992. Dynamics of phosphate head groups in biomembranes. Comprehensive analysis using phosphorus-31 nuclear magnetic resonance lineshape and relaxation time measurements. *Biophys. J.* 61:42–57.

46. Dufourc, E. J., J. F. Faucon, G. Fourche, J. Dufourcq, T. Gulik-Krywicki, and M. Le Maire. 1986. Reversible disc-to-vesicle transition of melittin-DPPC complexes triggered by the phospholipid acyl chain melting. *FEBS Lett.* 201:205–209.

47. Dufourc, E. J., I. C. P. Smith, and J. Dufourcq. 1986. Molecular details of melittin-induced lysis of phospholipid membranes as revealed by deuterium and phosphorus NMR. *Biochemistry.* 25:6448–6455.

48. Faucon, J. F., J. M. Bonmatin, J. Dufourcq, and E. J. Dufourc. 1995. Acyl chain length dependence in the stability of melittin-phosphatidylcholine complexes. A light scattering and ^{31}P-NMR study. *Biochim. Biophys. Acta.* 1234:235–243.

49. Pott, T., and E. J. Dufourc. 1995. Action of melittin on the DPPC-cholesterol liquid-ordered phase: a solid state ^{2}H and ^{31}P-NMR study. *Biophys. J.* 68:965–977.

50. Pott, T., M. Paternostre, and E. J. Dufourc. 1998. A comparative study of the action of melittin on sphingomyelin and phosphatidylcholine bilayers. *Eur. Biophys. J.* 27:237–245.

51. Carrillo, C., J. A. Teruel, F. J. Aranda, and A. Ortiz. 2003. Molecular mechanism of membrane permeabilization by the peptide antibiotic surfactin. *Biochim. Biophys. Acta.* 1611:91–97.

52. Grau, A., J. C. Gómez Fernández, F. Peypoux, and A. Ortiz. 1999. A study on the interactions of surfactin with phospholipid vesicles. *Biochim. Biophys. Acta.* 1418:307–319.

53. Marsh, D. 1990. CRC Handbook of Lipid Bilayers. CRC Press, Boca Raton, FL.

54. Maget-Dana, R., L. Thimon, F. Peypoux, and M. Ptak. 1992. Surfactin/iturin A interactions may explain the synergistic effect of surfactin on the biological properties of iturin A. *Biochimie.* 74:1047–1051.

55. Dufourc, E. J., E. J. Parish, S. Chitrakorn, and I. C. P. Smith. 1984. Structural and dynamical details of cholesterol lipid interaction as revealed by deuterium NMR. *Biochemistry.* 23:6062–6071.

56. Vist, M. R., and J. H. Davis. 1990. Phase equilibria of cholesterol/dipalmitoylphosphatidylcholine mixtures: ^{2}H nuclear magnetic resonance and differential scanning calorimetry. *Biochemistry.* 29:451–464.

57. Deleu, M., O. Bouffioux, H. Razafindralambo, M. Paquot, C. Hbid, P. Thonart, P. Jacques, and R. Brasseur. 2003. Interaction of surfactin with membranes: A computational approach. *Langmuir.* 19:3377–3385.

58. Shai, Y. 1999. Mechanism of the binding, insertion and destabilization of phospholipid bilayer membranes by alpha-helical antimicrobial and cell non-selective membrane-lytic peptides. *Biochim. Biophys. Acta.* 1462:55–70.

59. Shai, Y. 2002. Mode of action of membrane active antimicrobial peptides. *Biopolymers.* 66:236–248.